McIntosh et al., http://www.jcb.org/cgi/content/full/jcb.201209154/DC1

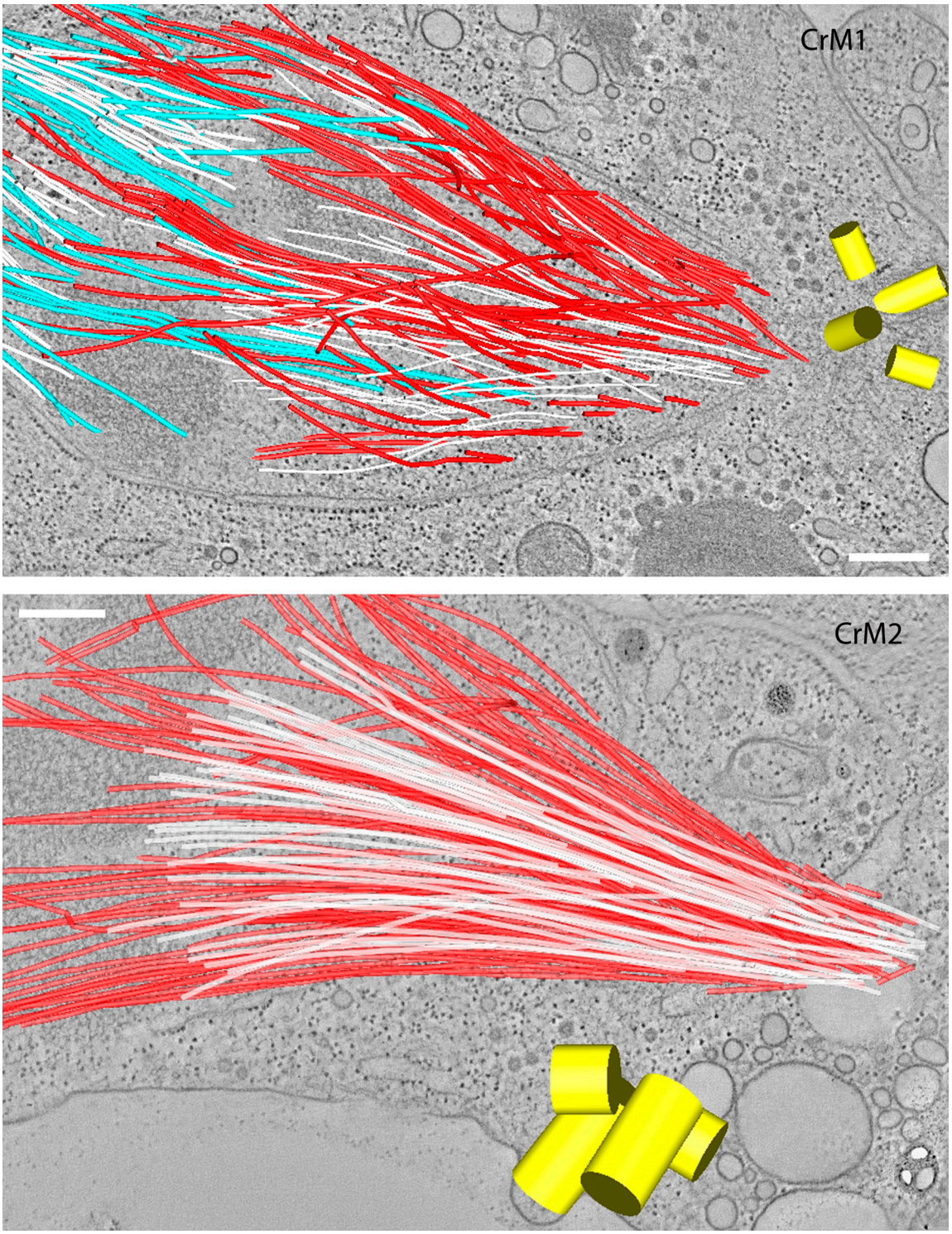

Figure S1. **Spindles from *C. reinhardtii* (Cr).** CrM1 and CrM2 are different metaphase cells. White lines indicate kinetochore-associated MTs, red and blue indicate non-KMTs from the two spindle poles. Yellow cylinders are centrioles. Models are superimposed on a tomographic slice from the 3D reconstruction. These cells were previously described by O'Toole et al. (2003). Bar, 500 nm.

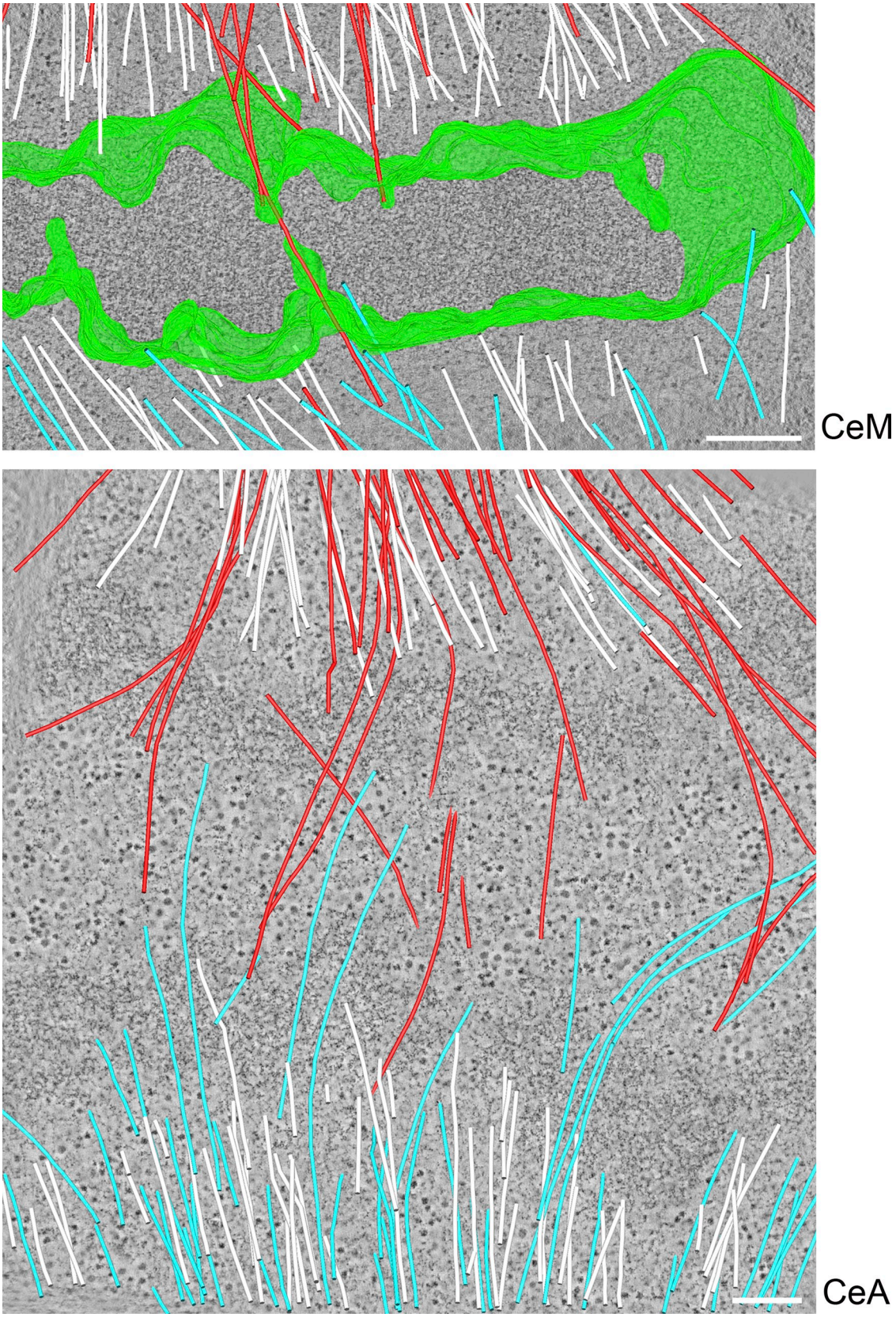

Figure S2. **Spindles from *C. elegans* (Ce).** CeM is a blastomere in metaphase and CeA is a similar cell in anaphase. White lines indicate KMTs, red and blue indicate non-KMTs. The green surface in CeM indicates the outline of the chromatin. Chromatin is visible in CeA as two masses without green outlines. These cells have been described previously by Muller-Reichert et al. (2008). Bars, 500 nm.

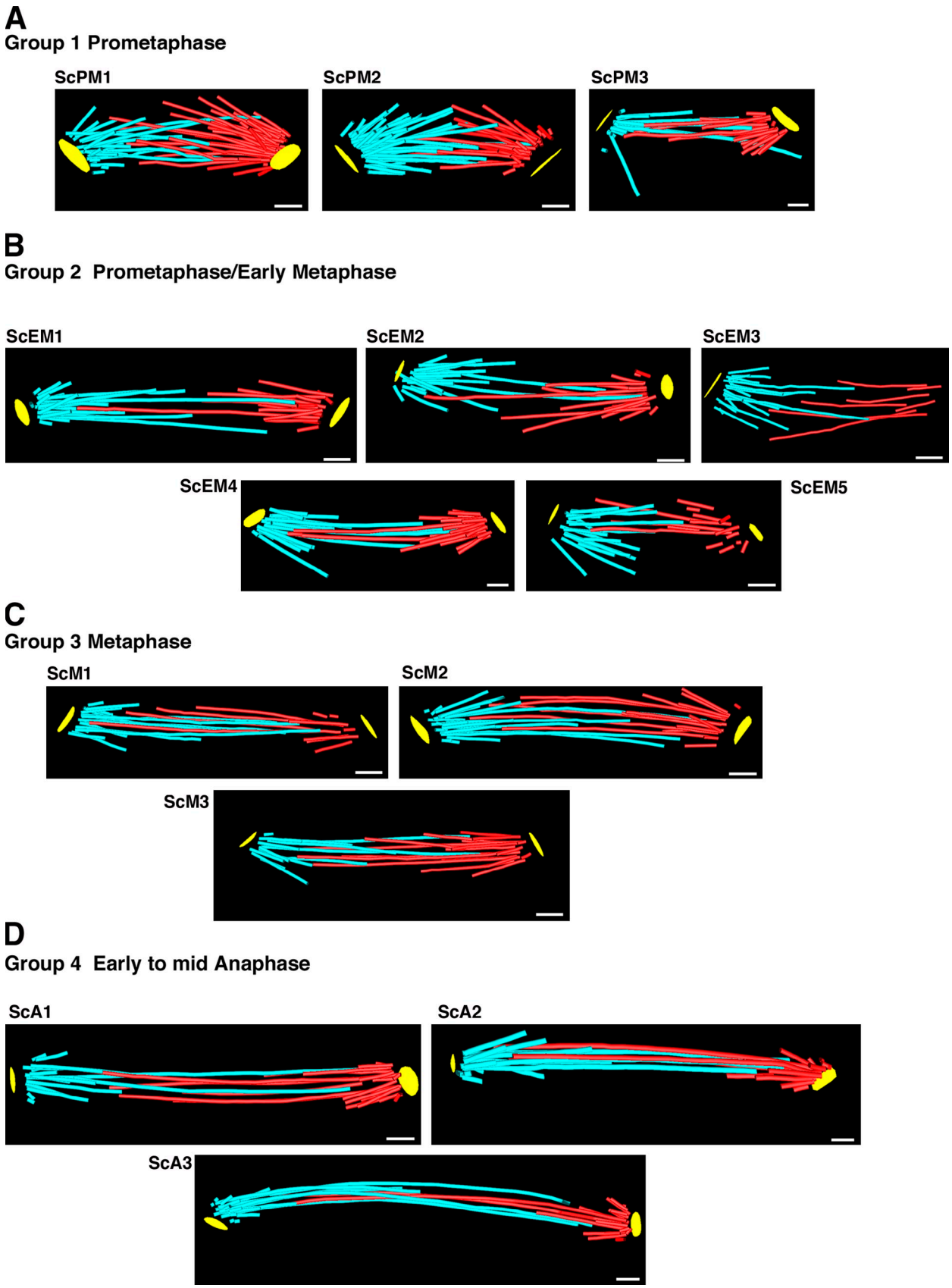

Figure S3. **Spindles from *S. cerevisiae* (Sc).** Panels show images of spindles at different stages of mitosis, as marked. Red and blue curves are MTs associated with the two spindle poles (yellow). Metaphase cells have been described previously by Gardner et al. (2008b); anaphase cells have been described previously by Gardner et al. (2008a). (A) Three spindles from cells in prometaphase. (B) Five spindles from cells in later prometaphase or early metaphase. (C) Three spindles from cells in metaphase. (D) Three spindles from cells in early to mid anaphase. Bars, 200 nm.

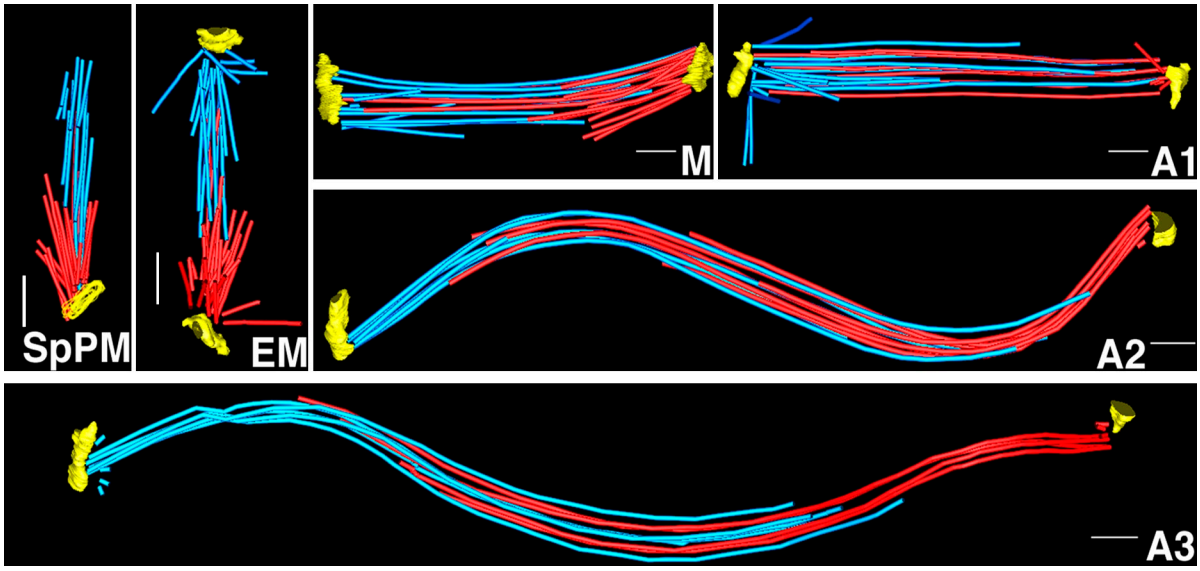

Figure S4. **Models of the *S. pombe* cells studied in this paper.** SpPM, *S. pombe* prometaphase; EM, early metaphase, late prometaphase; M, metaphase; A1, A2, and A3, anaphases 1, 2, and 3, which have been ordered on the basis of structure into a probable time series. Red and blue indicate MTs associated with one or the other spindle pole body. Yellow objects at spindle ends represent the spindle poles. The spindle shown as EM was previously described by Grishchuk et al. (2008). Bars, 200 nm.

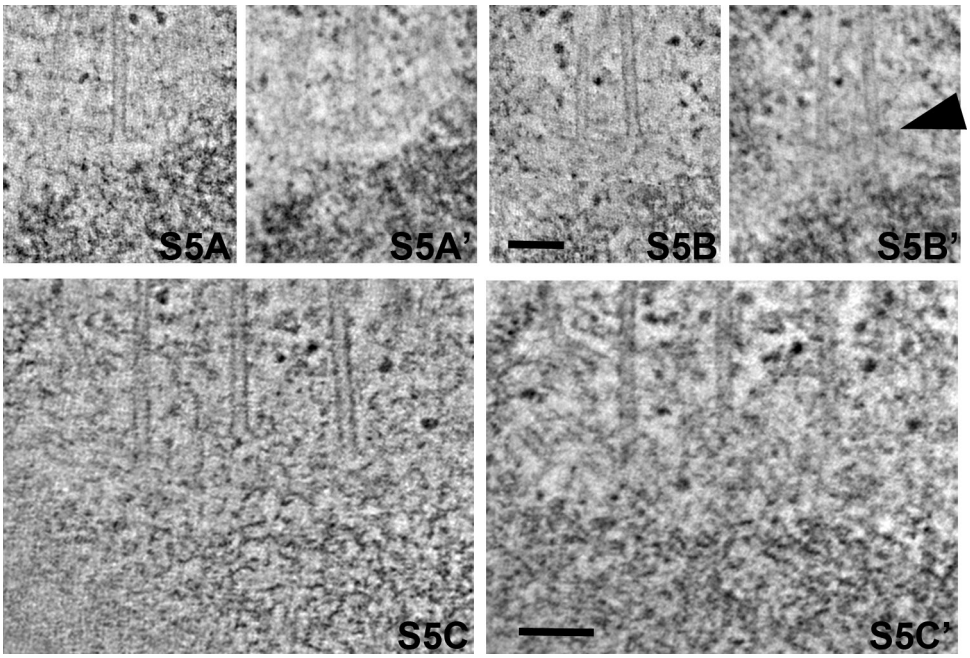

Figure S5. **Slices from tomograms of metaphase cells showing the effects of sample thickness on the appearance of the kinetochore–MT interface.** (A and B) KMTs from *C. reinhardtii* metaphase seen in tomographic slices 4 nm (A and B) or 25 nm thick (A′ and B′). The arrowhead marks an area that appears like an outer plate in the thicker sampling of the data. C (4 nm) and C′ (25 nm) show two views of the kinetochore region in *C. elegans*. No hint of an outer plate is seen at any thickness we have explored. Bars, 100 nm.

Table S1. **Conserved and divergent features of the kinetochore–MT interface**

I. Kinetochore organization at the interface with MT ends	
Conserved features	**Divergent features**
General structure of interface: fibrous meshwork with no conspicuous repetitive units or laminar arrangement	MTs terminate at various distances from the identifiable heterochromatin (in cells with sufficient chromatin condensation to make chromatin evident)
Lack of dense structures or "sleeves" surrounding the MT walls or ends	Yeast centromeres display specialized micro-structures (most likely based on one or more centromere-specific nucleosome); centromeric chromatin in other species is indistinguishable from surrounding chromatin
Similar appearances in cells with different numbers of KMTs, different kinetochore sizes and locations (e.g., holocentric vs. not)	Yeast KMT walls, close to the polymer plus ends, are surrounded by complete or partial rings
Fibrils connect flaring PFs with nearby chromatin or kinetochore meshwork, although the clarity and lengths of these structures are variable	
II. Fine structure of PFs at KMT ends	
Conserved features	**Divergent features**
The plus ends of all KMT ends display at least some flaring PFs	Average lengths of curving segments on KMT PFs differ; shortest PFs found in yeast.
There is little change in the average shapes of KMT plus ends during mitotic progression	Fraction of "ram's horns" PFs varies significantly and is highest in yeast
Elongated, gently curved PF "extensions" are rarity in cells	"Intermediate" PFs change their shapes during mitotic progression to a different degree[b]
KMT ends frequently contain PFs with "intermediate" shape, although their proportion varies among species, with the highest being in mammalian cells. These shapes are likely to result from modifications by both PF-associated MT-associated proteins and force-transducing links	
In all organisms there are factors that straighten the distal portions of all PFs, even the "ram's horns"	
KMT PFs are longer than PFs on non-kinetochore MTs, and they elongate in anaphase[a]	

[a]Data are weak in fission yeast and unavailable in budding yeast because of the brief duration of anaphase A and because their spindles contain few non-kinetochore MTs, except those that form interdigitating bundles (ipMTs).
[b]Results for yeasts are inconclusive because their PFs are too short for this analysis.

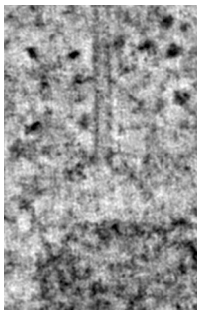

Video 1. **A KMT plus end from the *C. reinhardtii* metaphase cell CrM1.** A movie of 58 tomographic slices, each ~4 nm thick and all of which contained the MT axis, though they differed in orientation by 2°. Chromatin is the darkly staining material near the bottom of the images. The MT end is evident, as are many flaring PFs. Kinetochore fibrils can be seen associated with several of these PFs. To the left of the KMT, a non-KMT comes in and out of view as the plane rotates; to the right one can briefly see another KMT that is slightly oblique to the one under study. Darkly staining densities in the body of the spindle are probably ribonucleoprotein particles. On the left side of the MT a fiber runs almost parallel to the MT near its plus end; it seems to associate with the MT wall. This is one of our best examples of a fibril interacting with a KMT wall. Although the quality of these images is not quite as good as that of the original tomogram, this video provides a good representation of the raw data upon which the identification and characterization of PFs and fibrils were based.

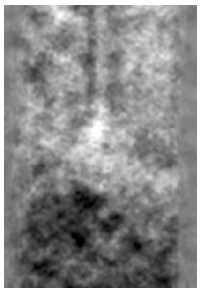

Video 2. **Average of KMTs from the *C. reinhardtii* cell CrM1.** A movie of 66 axial slices, made as described for Video 1, but using the average of 29 aligned KMTs prepared with PEET (see Materials and methods). The MT walls are still strong image features, because they were used for alignment, and chromatin is still dark, because it is uniformly well stained, even if its local structure is heterogeneous. Background staining in the spindle is blurred by the averaging, so the darkly staining particles that are obvious in Video 1 are largely invisible here. In the region between the flaring PFs and the chromatin, however, one can still see indications of fibrils. Given the blurring of nucleoplasm seen elsewhere, these features are surprising. Some fibrils appear to bind to flaring PFs quite close to the straight part of the MT wall, and some bind farther out. The way in which fibrils emerge during averaging can be seen in the Fig. 7. Most fibrils are, however, not placed similarly on the multiple MTs in the average, so they do not reinforce.

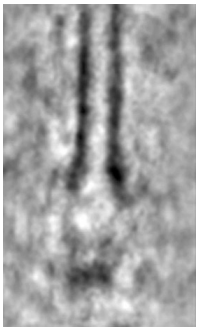

Video 3. **Average of KMTs from the *S. cerevisiae* cell ScM3.** A movie of 66 axial slices from the average of 18 metaphase KMTs, as described for Video 2. In this cell, the nucleoplasm was sufficiently clear and the MT walls were sufficiently strong that no masking was necessary to help PEET obtain a good image alignment. In this cell, the density ~50 nm from the MT end is particularly clear, although the apparent shape of its average is not a simple toroid, which suggests that the azimuthal orientations of these "kinetochores" were not aligned. The averaging has blurred most nucleoplasmic features, but there are indications of quite a few fibrils connecting the toroidal density with the flared MT ends.

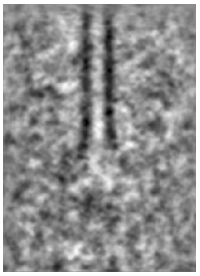

Video 4. **Average of KMTs from *S. pombe* cell SpEM.** A movie of 53 axial slices from the average of 18 KMTs, as described for Video 2. The nucleoplasm in this well-fixed fission yeast cell is particularly dense, but in the average a density is evident, ~50 nm from the end of the averaged MT. Some views suggest the presence of a toroidal structure, as if the density contained one or more nucleosomes, but it is larger and less well-defined than the density seen in budding yeast. There are hints of fibrils in some orientations, but they are not as clear as in budding yeast.

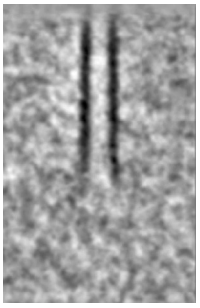

Video 5. **Average of non-KMTs from the *S. pombe* cell SpEM.** A movie of 51 axial slices from the average of 15 non-KMTs, as described in Video 2. Here the MT walls are clear in all orientations, but there are no special densities near the MT end. One occasionally catches a glimpse of a toroidal structure, but such objects are seen in many regions of the nucleoplasm, including beside the MT wall in these averages. The density seen in Video 4 seems, therefore, to be particular to the ends of KMTs.

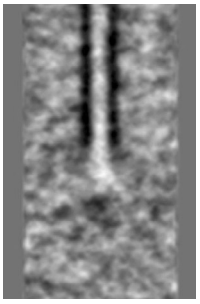

Video 6. **Average of all available KMTs from preanaphase *S. pombe* cells.** Because the MT end-associated density in Video 4 is ill-defined, we normalized the magnifications of all preanaphase fission yeast tomograms and extracted their 38 KMTs to average with PEET. The larger number of elements in the average produced a better signal-to-noise ratio for the MT walls, and it also enhanced a density ~50 nm from the average MT end. Now the density has apparent substructure, such as a dark center and radial arms, some of which appear to extend as far as nearby PFs. The presence of a density near KMT ends is thereby confirmed, but its exact structure is ill-defined.

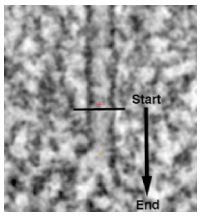

Video 7. **Cross sections of a budding yeast KMT near its plus end.** Here we take advantage of the 3D structure of a tomogram to view a prometaphase KMT from a budding yeast cell (ScPM2) from two orthogonal orientations: looking perpendicular to, then parallel to, the MT axis. The 53 frames of the video are best viewed by stepping through them one by one, rather than by letting the movie run. Frame 1 presents the MT view seen throughout this paper; a red plus sign marks the place on the MT axis from which cross-sectional viewing will begin on frame 2. Successive frames then march in ~2-nm steps to the MT plus end and then on into the nucleoplasm beyond the MT. The red plus sign tracks the MT lumen. The faint yellow plus sign that appears occasionally has no significance. The last two frames are tipped back up to the initial view, and again the red plus shows where the last cross section was taken, just above a putative kinetochore. Frame 30 cuts the MT at about the place where the PFs begin to flare out, and subsequent steps show the obvious widening of the MT lumen and multiple PFs flare. Frame 13 shows evidence for a limitation of tomograms; the MT wall just above the red plus appears to herniate. We interpret this image as a smearing of density along the beam axis (vertical on this view), which has led to the apparent fusion of a darkly staining nucleoplasmic particle with the wall of the MT. Alternative possibilities are that this MT was not well preserved by rapid freezing/freeze substitution, or that this is an accurate representation of an abnormality in the MT wall. By frame 24, the MT has become normal again. In the region of frames 26–30, there are examples of partial ringlike structures on the left side of the MT. To the left of the MT marked with the red plus there are two MTs that end sooner in C-shaped structures, indicating that not all PFs terminated at the same place along the MT axis. To the right of the marked MT there is another that continues to the end of the sequence, albeit indistinctly. These views show both strengths and weaknesses of tomograms. The ability to view the same volume from multiple orientations is valuable, but the lack of isotropy in the image's line-spread function makes features indistinct when viewed from an angle that exposes the loss of information, given the missing pyramid of data that results from the limitation on maximal tilt.

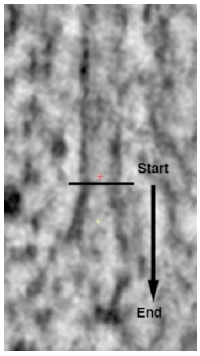

Video 8. **Cross sections of a budding yeast KMT near its plus end.** A 69-frame video of a KMT from ScM3, analogous to Video 7, with the first and last images showing the places along the MT axis where the cross-sectional series begins and ends. The red plus sign tracks the MT lumen. The faint yellow plus sign that appears occasionally has no significance. At frames 9–12, there is a partial ring on the right side of the marked MT. At around frame 18, the MT begins to end; there are some PFs that seem to stop without flaring, leading to an incomplete MT wall. The other PFs then flare as usual. Some PFs are longer than others, and additional material appears to connect the flaring PFs with the KMT-associated density seen near the end of the movie.

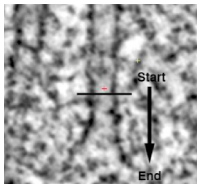

Video 9. **Cross sections of a fission yeast KMT near its plus end.** A 69-frame video analogous to Video 8; again red plus signs show on the first and last frames to show the paraxial distance covered by the cross sections and to track the MT lumen. The faint yellow plus sign that appears occasionally has no significance. A KMT from SpEM is tracked through its end and into the chromatin density described in the text. The MT diameter starts to increase around frame 25, forming a rather symmetrical flared end. A partial ring is visible on the left around frame 22. At frame 64, a clear toroid is visible on the MT axis, which may be part of the fission yeast kinetochore.

References

Gardner, M.K., D.C. Bouck, L.V. Paliulis, J.B. Meehl, E.T. O'Toole, J. Haase, A. Soubry, A.P. Joglekar, M. Winey, E.D. Salmon, et al. 2008a. Chromosome congression by Kinesin-5 motor-mediated disassembly of longer kinetochore microtubules. *Cell*. 135:894–906. http://dx.doi.org/10.1016/j.cell.2008.09.046

Gardner, M.K., J. Haase, K. Mythreye, J.N. Molk, M. Anderson, A.P. Joglekar, E.T. O'Toole, M. Winey, E.D. Salmon, D.J. Odde, and K. Bloom. 2008b. The microtubule-based motor Kar3 and plus end-binding protein Bim1 provide structural support for the anaphase spindle. *J. Cell Biol.* 180:91–100. http://dx.doi.org/10.1083/jcb.200710164

Grishchuk, E.L., A.K. Efremov, V.A. Volkov, I.S. Spiridonov, N. Gudimchuk, S. Westermann, D. Drubin, G. Barnes, J.R. McIntosh, and F.I. Ataullakhanov. 2008. The Dam1 ring binds microtubules strongly enough to be a processive as well as energy-efficient coupler for chromosome motion. *Proc. Natl. Acad. Sci. USA*. 105:15423–15428. http://dx.doi.org/10.1073/pnas.0807859105

Müller-Reichert, T., J. Mäntler, M. Srayko, and E. O'Toole. 2008. Electron microscopy of the early *Caenorhabditis elegans* embryo. *J. Microsc.* 230:297–307. http://dx.doi.org/10.1111/j.1365-2818.2008.01985.x

O'Toole, E.T., T.H. Giddings, J.R. McIntosh, and S.K. Dutcher. 2003. Three-dimensional organization of basal bodies from wild-type and delta-tubulin deletion strains of *Chlamydomonas reinhardtii*. *Mol. Biol. Cell*. 14:2999–3012. http://dx.doi.org/10.1091/mbc.E02-11-0755